Journal of Alloys and Compounds 509 (2011) 2758–2769

Contents lists available at ScienceDirect

Journal of Alloys and Compounds

journal homepage: www.elsevier.com/locate/jallcom

Optimization of friction welding of tube to tube plate using an external tool by hybrid approach

S. Senthil Kumaran [a], S. Muthukumaran [a,*], S. Vinodh [b]

[a] Department of Metallurgical and Materials Engineering, National Institute of Technology, Tiruchirappalli 620015, Tamil Nadu, India
[b] Department of Production Engineering, National Institute of Technology, Tiruchirappalli 620015, Tamil Nadu, India

ARTICLE INFO

Article history:
Received 23 October 2010
Accepted 10 November 2010
Available online 18 November 2010

Keywords:
Friction welding
Tube to tube plate
Artificial Neural Network
Genetic Algorithm
ANOVA

ABSTRACT

Several developments have been observed in the field of materials processing and welding is a vital metal joining process that has potential industrial applications. Friction welding of tube to tube plate using an external tool (FWTPET) is a relatively newer solid state welding process used for joining tube to tube plate of either similar or dissimilar materials with enhanced mechanical and metallurgical properties. Generally, welding is a multi-input and multi-output process in which there exists a close relationship between the quality of joints and the welding parameters. In the present study, Artificial Neural Network (ANN) has been used to predict the strength behavior of FWTPET process. Several Neural Network architectures have been subjected to analysis and the optimal architecture has been determined. The optimal architecture has been used to predict the output process parameter. The predicted output and input parameters have been optimized using Genetic Algorithm (GA). GA optimized and experimentally determined process parameters were compared and the deviation is found to be minimal. Besides, the most influential process parameter has been determined using statistical analysis of variance (ANOVA).

1. Introduction

An overview on solid state welding current literature indicate that, the research in friction welding has been reported only from the perspective of joining rod to rod/tube to tube; however there is little evidence of joining tube to tube plate by the available solid state methods. In this context, Friction welding of tube to tube plate using an external tool (FWTPET) process is capable of joining tube to tube plate which is an innovative as well as adds knowledge to the contemporary solid state welding methods. FWTPET was invented in the year 2006 by one of the present authors [1]. This is a relatively new solid state welding process used for joining tube to tube plate of either similar or dissimilar materials with enhanced mechanical properties such as hardness and tensile strength. Some of the important process parameters of FWTPET considered is tool rotational speed, shoulder diameter and clearance between pin and tube. Significant improvement in metallurgical and mechanical properties of FWTPET process depends on the efficient control of its process parameters. Senthil Kumaran et al. discussed about Taguchi L8 orthogonal array in the previous investigation of tube to tube plate welding using an external tool and the statistical significance of the welding process parameters has been determined by the conduct of ANOVA [2]. Senthil Kumaran et al. investigated for using the configurations with and without backing block and the results of post processing revealed that the configuration with backing block is characterized with lesser stress, minimum deformation and comparatively lesser strains by FEA employing ABAQUS package [3]. In order to produce good quality weld joints, it is vital to set proper welding process parameters. Generally, the welding process is characterized with close relationship between the quality of joints and the welding parameters. This process of identification of suitable combination of input process parameters so as to produce the desired output parameters necessitates the conduct of several experiments which consumes time and cost. Several efforts have been investigated to understand the effect of process parameters on material flow behavior, microstructure formation and mechanical properties of friction welded joints [4]. In order to investigate the effect of friction welding process parameters, most researchers follow the conventional experimental techniques wherein one parameter will be varied over a period of time whereas other parameters are kept constant [2]. This kind of conventional parameter based design of experiment approach is time consuming and consumes enormous amount of resources [5].

In this context, modeling is necessary to understand and control any process. In recent years, Artificial Neural Network (ANN) is one of the most powerful modeling facilities currently being used in many engineering fields of engineering for modeling complex relationships which are difficult to be described with physical models [5]. Further, the literature review reveals that there has been scant research undertaken on the use of ANNs in predicting

* Corresponding author. Mobile: +91 9442069381; fax: +91 431 2500133.
E-mail address: smuthu@nitt.edu (S. Muthukumaran).

0925-8388/$ – see front matter © 2010 Elsevier B.V. All rights reserved.
doi:10.1016/j.jallcom.2010.11.067

strength behavior of welding process under different conditions. In this study, a hybrid approach involving the usage of ANN for generating the optimal architecture and Genetic Algorithm (GA) for optimizing the process parameters has been deployed. This hybrid approach overcomes the drawbacks associated with single optimization tools/techniques. Hence, in this study, an attempt has been made to apply ANN approach to develop a well correlated model which predicts the tensile strength behavior of FWTPET process under different conditions by considering the tool rotational speed, pin clearance and shoulder diameter as input neurons for ANN model. The experimental results of the tensile strength are designated as output neurons in the model. The optimal architecture has been determined. The optimal architecture has been used for providing inputs to GA. The optimized input and output parameters generated by GA has been compared with experimentally determined values. This is followed by the conduct of ANOVA for ensuring the statistical significance of the process parameters.

2. FWTPET process

The FWTPET machine developed in-house is shown in Fig. 1. The external tool consists of a shoulder and pin which is shown in Fig. 2(a). The tube to tube weld is cleaned and holes are prepared along the faying surfaces of the tube. A suitable hole is drilled in a plate and the tube is fitted and then assembled in FWTPET machine table. FWTPET machine includes of tool holder, spindle, table and supporting structure. The tool is lowered during rotation and heat is generated due to friction when the shoulder touches the plate. The plastic flow of metal takes place towards the center of the tool axis [3]. The metal flows through the holes in the tube and occupies the gap between pin and inner diameter of the tube as shown in Fig. 2(b). The tool is withdrawn after predetermined time. The cylindrical pin restricts the material movement and pressure is applied between the tube and plate. The bonding occurs between surfaces which are at higher pressure and temperature [6]. The process variables considered in this research study are tool rotational speed, pin clearance and shoulder diameter. Both the tube and plate used in the present study are made of commercial grade pure aluminium whose chemical composition is shown in Table 1. The experiment has been conducted using 6 mm rolled plates of commercial grade pure aluminium and cut into the required sizes (50 mm × 70 mm) by means of a power hacksaw. Similarly, tubes of 16 mm external diameter have been cut into required size (35 mm height).

Fig. 1. FWTPET machine (developed in-house).

This is followed by drilling of 16 mm diameter holes in the rolled plate. Then the tubes are fixed in their respective hole position. Tools made of tool steel are used to fabricate FWTPET joints in the present study. The assembled work piece is clamped on to the machine table and the tool has been fixed to the spindle of the machine. FWTPET weld joint before and after friction welding process are shown in Figs. 3 and 4 respectively. On completion of welding, the tube to tube plate joints are sliced for macro-structural observation. The rough scratches on the surfaces have been removed using a belt grinder. The fine scratches have been removed using emery sheet of different grades and further polishing has been performed using alumina and diamond paste by employing a disc polishing machine. This is followed by etching the macro-structure using tucker's reagent (composition: 4.5 ml HNO_3, 2.5 ml H_2O, 1.5 ml HCl, 1.5 ml HF). Then the sample has been washed, dried and observed using a macroscope.

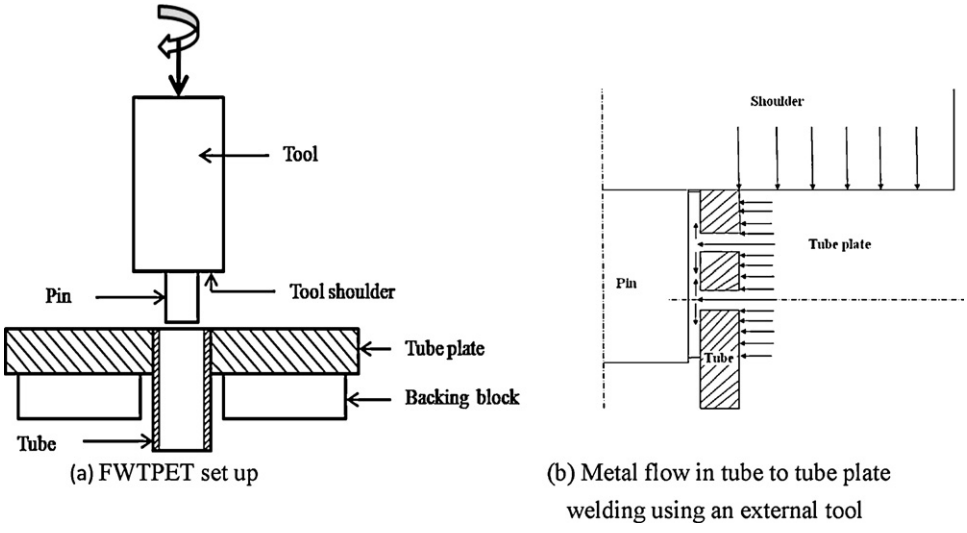

Fig. 2. FWTPET process description. (a) FWTPET set up and (b) metal flow in tube to tube plate welding using an external tool.

Table 1
Chemical composition of parent metal.

	Element									
	Al	Si	Fe	Cu	Mg	Mn	Ti	Zn	Cr	V
Wt %	Bal	0.0006	0.0007	0.0013	0.0021	0.0001	0.0001	0.0002	0.0001	0.0001

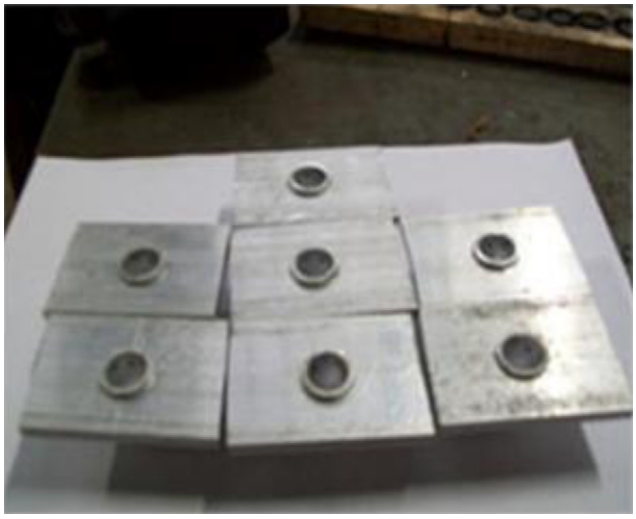

Fig. 3. Arrangement of tube to tube plate before FWTPET process.

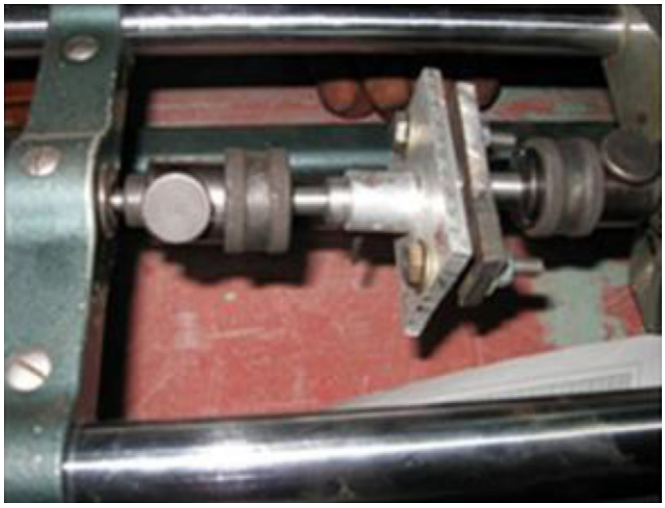

Fig. 5. Tensile test conducted using a tensometer.

2.1. Microstructural study

The microstructural aspects of the friction welded joints are studied through optical microscopy. The integrity of joints has been analyzed through micrographs at the weld zone. The Keller's etchant has been used for microstructural studies (composition: 2 ml HF, 3 ml HCl, 5 ml HNO_3, 190 ml distilled water).

2.2. Tensile test

Tensile test is conducted using a tensometer for the joints fabricated using FWTPET process. Tensile test specimen has been fixed in the tensometer is shown in Fig. 5. Three joints have been tested for each set of processing parameters and the mean value is obtained.

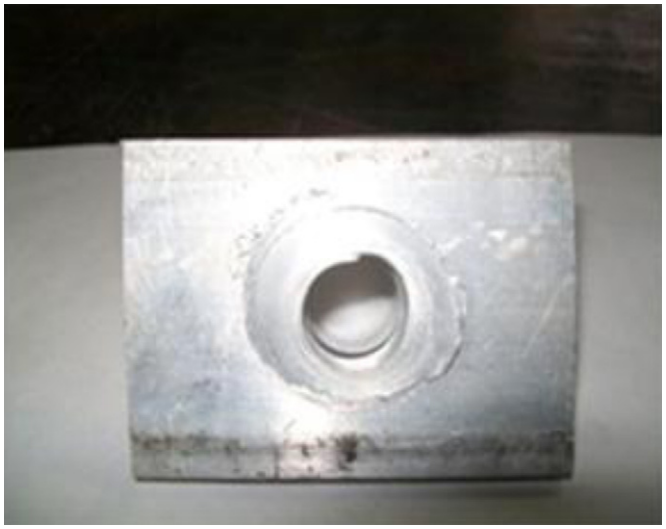

Fig. 4. Tube to tube plate weld joints after FWTPET process.

3. Artificial Neural Networks

Neural networks, working on the principle of artificial intelligence, have traditionally been viewed as simplified models of neurons in the human brain. It is accepted globally that the human brain performs excessive computations. The origin of neural networks have been traced to information processing model in biological systems, which is based on parallel processing as well as implicit instructions of "sensory" input from external sources [7].

3.1. Backpropagation neural network (BPNN)

The backpropagation (BP) algorithm is capable of designing multi-layer neural networks for numerous applications, such as adaptive control, classification of sonar targets, stock market prediction and speech recognition [8]. Also, BPNN possess the advantage of fast response and high learning accuracy [9]. Hence an ANN with backpropagation algorithm (BP) has been adopted in our study to model the strength behavior of FWTPET process. One of the advantages is that the model can be constructed very easily based on the input and output data and trained to accurately predict the process dynamics. This technique is especially valuable in processes where a complete understanding of the physical mechanisms is very difficult, as in the case of measuring tensile strength during welding. Neural network is a logical structure with multi-processing elements, which are connected through interconnection weights. The knowledge is presented by the interconnection weights, which can be adjusted during the learning phase. There are several algorithms available among which the Levenberg–Marquardt algorithm (trainlm) is characterized by fastest convergence [10,11]. In many cases, trainlm is capable of obtaining lower mean square errors than its counterparts. This BP network possesses a multi-layer network architecture including the input layer, hidden layer(s) and output layer. Layers include several processing units known as neurons. In the network, the input layer receives information from external source and passes this information to the network for processing. The hidden layers

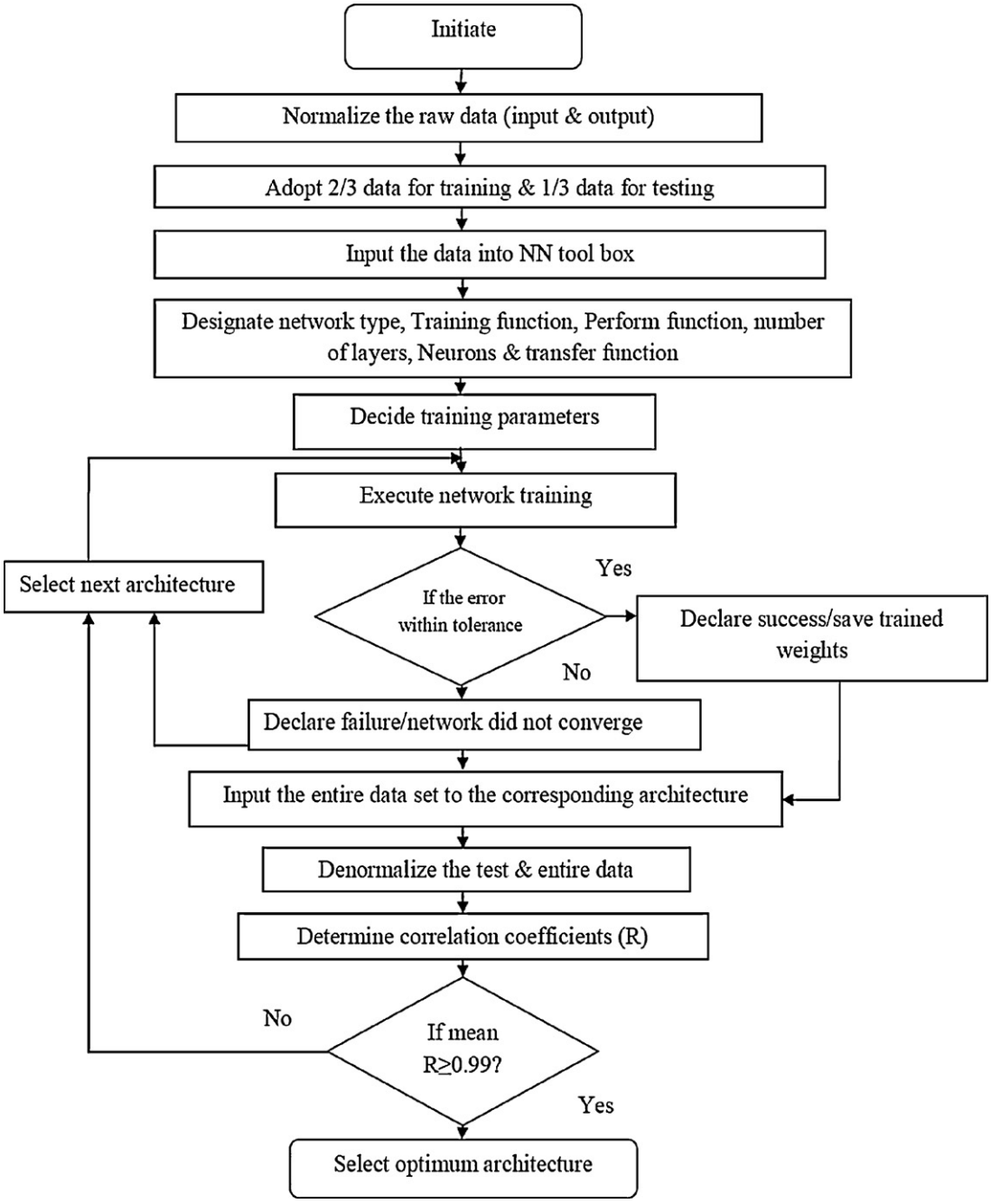

Fig. 6. Sequence of steps in NN algorithm.

receive data from the input layer, and perform information processing. The output layer receives processed information from the network, and sends the results to an external receptor [12]. The BP algorithm is shown in Fig. 6.

3.2. Model description

In the development of a multi-layer neural network model, some decisions to be made include number of neuron(s) in the input layer, number of hidden layer(s), number of neuron(s) in the hidden layer(s), and number of neuron(s) in the output layer and optimum architecture. The input parameters are the tool rotational speed, pin clearance and shoulder diameter. The output parameter is the tensile strength. The input/output dataset of the model is illustrated schematically in Fig. 7.

3.2.1. Data normalization

Higher valued input variables may tend to suppress the influence of smaller ones. To overcome this problem, the neural network has been trained using the normalized input data, leaving it to the network to learn weights associated with the connections emanating from these inputs. The raw data are scaled in the range −1 to +1 for use by neural networks to minimize the effects of magnitude between inputs and also aids the backpropagation learning algorithm. The normalized values (X_n) for each raw input/output dataset (d_i) was computed as

$$x_n = \frac{2(d_i - d_{\min})}{d_{\max} - d_{\min}} - 1 \quad (1)$$

where $d_{\max}$ and $d_{\min}$ are the maximum and the minimum values of raw data.

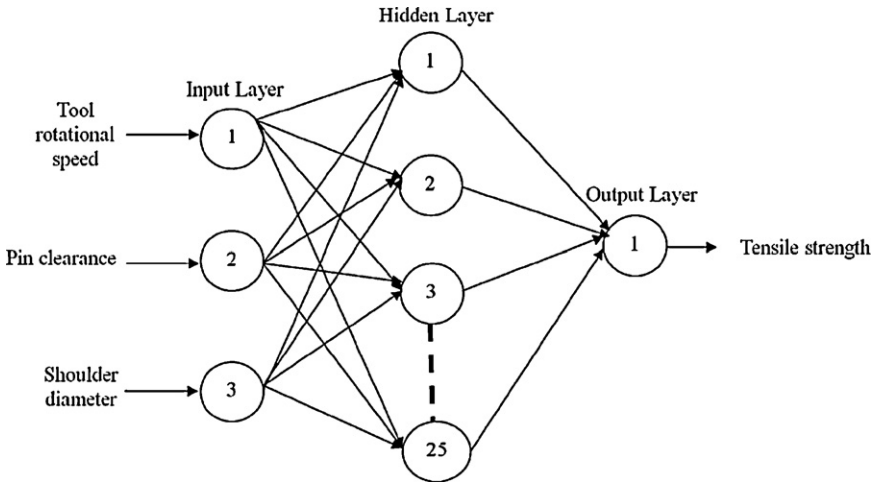

Fig. 7. Architecture of ANN model employed in our study.

3.2.2. Neural network design and training

In this model, three imperative input parameters used are the tool rotational speed, pin clearance and shoulder diameter, while the output parameter is the tensile strength. In this study, the total number of experimental results is 27 ($27 \times 1 = 27$) dataset among which 18 (two-third) data has been utilized for training, and 9 (one-third) data has been used for testing. Before training the network, the input/output dataset were normalized within the range of ± 1 using Eq. (1). The standard multi-layer feed forward backpropagation hierarchical neural networks were designed using MATLAB 7.5 Neural Network Toolbox. The network consists of three layers: the input, hidden layer, and output layers. Now, the designed network has three input neurons and one output neuron. In the network, each neuron receives total input from all of the neurons in the proceeding layer as:

$$net_j = \sum_i W_{ji}^n (x_i)^{n-1} \tag{2}$$

where net_j is the total or net input, $x_i{}^n$ is the output of the node j in the nth layer, and W_{ji}^n represents the weights from node i in the $(n-1)$th layer to node j in the nth layer. A neuron in the network produces its output by processing the net input through a non-linear activation function. There are several types of activation functions used for BP. However, the tan–sigmoid transfer function is mostly used which is assigned in hidden layer(s) for processing the inputs as:

$$f_{(x)} = \left(\frac{e^x - e^{-x}}{e^x + e^{-x}} \right) - 1 \quad \text{range } (-1, 1) \tag{3}$$

and purelin is a transfer function calculating a hidden layer's output from its net input which is assigned for output layer as:

$$f_{(x)} - \frac{2}{1 + e^{-x}} - 1 \quad \text{range } (-1, 1) \tag{4}$$

The weights are dynamically updated using the BP algorithm. The network has been trained with Levenberg–Marquardt algorithm. This training algorithm is selected due to its high accuracy in similar function approximation [13]. In order to judge the performance of the network, the average error (MSE) has been used which is obtained by:

$$E_p = \sum_{p=1}^{p} \sum_{k=1}^{k} (d_{pk} - o_{pk}) \tag{5}$$

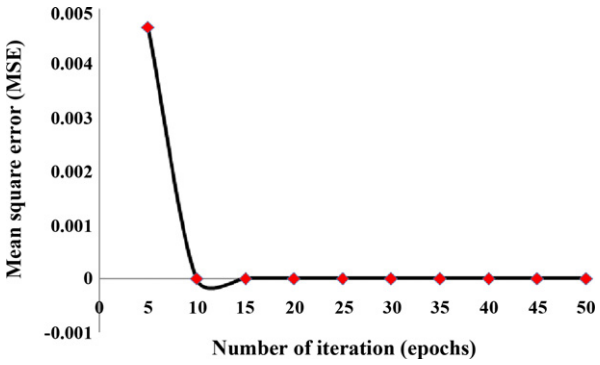

Fig. 8. Variation of the MSE of the trained data as a function of epochs for (3–10–1) ANN Architecture.

where d_{pk} and o_{pk} are the desired and calculated output for kth response, respectively. 'k' denotes the number of neurons in output of network and and 'p' is the total number of instances (epochs). The number of iterations (epochs) to be executed is an important parameter in the case of BPNN training [14]. Initially, three neurons in input layer, 10 hidden neurons each in one hidden layers and one neurons in output layer (3–10–1) architecture has been designed and trained with different number of epochs to determine the optimum iterations. The MSE achieved from different iterations is shown in Fig. 8. It is evident that the value of MSE gradually decreases during the progress of training. An error of $3.23e^{-28}$ at 15 epochs is reduced to $1.45e^{-21}$ after 25 iterations and not much change has been observed with further iterations. The training parameter used in our model is presented in Table 2.

The action of determining the optimal number of hidden neurons is a crucial step. The number of hidden neurons must be

Table 2
Training parameters used in the model.

Trainlm's training parameters	Value
Maximum number of epochs to train	25
Performance goal	0
Maximum validation failures	5
Factors to use for memory/speed tradeoff	1
Minimum performance	$1e^{-10}$
Initial μ (scalar)	0.001
μ decrease factor	1
Maximum μ	$1e^{10}$
Epochs between displays	25
Maximum time to train in seconds	Infinity

sufficiently large to realize certain function. Several structures have to be considered with different numbers of hidden neurons to determine the best configuration [15]. The strength behavior of FWTPET process under different conditions has been trained with different architectures by varying number of neurons in the hidden layer(s). After training, it has been denormalized and compared with the experimental data. The denormalized values (x_i) for each raw output dataset was calculated as

$$x_i = \frac{(X_n + 1)(d_{\max} - d_{\min})}{2} + d_{\min} \quad (6)$$

where $d_{\max}$ and $d_{\min}$ are the maximum and the minimum values of raw data.

For testing the prediction ability of the model, prediction error in each output node has been calculated as follows:

$$Prediction\ \ error\ \ \% = \frac{Actual\ \ value - Predicted\ \ value}{Actual\ \ value} \times 100 \quad (7)$$

In order to determine the optimal architecture, totally 35 different networks with different number of layers and neurons in the hidden layer have been designed and tested for their validity of strength behavior of FWTPET process.

4. Genetic Algorithm

Genetic Algorithm (GA) is a nontraditional optimization algorithm based on the principle 'Fit parents would yield fit offspring'. GA has wide variety of applications in engineering problems because of simplicity and ease of operation [16]. GA is a computerized search and optimization algorithm based on the mechanics of natural genetics and natural selection. According to Darwin's natural selection theory, strong individuals of a population survive, while weak individuals do not. The surviving individuals mate to produce the next generation of individuals. It is clear that individuals in the next generation will be better than the individuals of the previous generations; individuals continue to get fitter as evolution continues. Thus, individuals ultimately become perfect [17]. GA is an evolutionary optimization method that uses a group of initial solutions. These solutions are represented by the design variables. GA improves these solutions by using certain genetic rules. The initial population is randomly determined. This step of generation of solutions is taken to be the first generation of the design, and each individual is considered to be a solution within a given generation. The solutions for each generation are coded using binary numbers in order that genetic operators can be readily applied. After determining the initial population, the genetic evolution begins. At first, the fitness of each individual is determined according to their closeness to the optimum solution, and individuals are categorized according to their fitness. After that, the reproduction, crossover and mutation operators are applied to each generation to evolve a new generation. This evolution continues until the majority of the solutions are identical [18] i.e. the convergence has occurred. The minimum or maximum of a function is determined based on the variation of $X_1, X_2, X_3, \ldots, X_n$ beginning with one or more starting point. GA generally evaluates a set of points, and the basic elements of GA consist of a chromosome and fitness value. The fitness value describes how well an individual can adapt to survival and mating. In our project, the basic element of GA consists of values of speed, pin clearance, shoulder diameter and tensile strength [f(S, PC, SD)]. GA works on the basis of binary code in the form of 0 and 1. An individual in GA is denoted by I [{S, PC, SD, f(S, PC, SD)}]. A set of search individual is called a population. The objective function is given by tensile strength [f(S, PC, SD)]. The parameters used in GA and their values are shown in Table 3.

Table 3
Parameters and their values used in GA.

Parameters	Values
Population size	100
Length of chromosome	20
Selection operator	Stochastic uniform
Crossover probability	0.8
Mutation probability	0.2
Fitness parameter	Tensile strength

4.1. Welding constraint

The practical constraints imposed during welding process are stated as follows:

Parameter bounds:

Bounds on tool rotational speed (S)

$$S_L \le S \le S_H$$

where S_L = 500 rpm and S_H = 1500 rpm are least and highest speed respectively.

Bounds on pin clearance (PC)

$$PC_L \le PC \le PC_H$$

where PC_L = 1 mm and PC_H = 3 mm are least and highest pin clearance respectively.

Bounds on shoulder diameter (SD)

$$SD_L \le SD \le SD_H$$

where SD_L = 20 mm and SD_H = 30 mm are least and highest shoulder diameter respectively.

The problem of GA has been solved using MATLAB.

5. Statistical technique

The purpose of the statistical analysis of variance (ANOVA) is to investigate which of the process parameters significantly affect the performance characteristics. ANOVA and *F*-test are used to analyze the experimental data. Minitab (version 15) software is used to analyze the collected data.

$$S_m = \frac{(\Sigma \eta_i)^2}{16} \quad (8)$$

$$S_T = \Sigma \eta^2 - S_m \quad (9)$$

$$S_A = \frac{(\Sigma \eta^2 A_i)^2}{N} - S_m \quad (10)$$

$$S_E = S_T - \Sigma S_A \quad (11)$$

$$V_A = \frac{S_A}{f_A} \quad (12)$$

$$F_{A_0} = \frac{V_A}{V_E} \quad (13)$$

where S_T is the sum of squares due to the total variation, S_m the sum of squares due to the mean, S_A the sum of squares due to parameter A (A is tool rotational speed), S_E the sum of squares due to error, η_i the output value of each experiment (i = 1,.. . ., 16), η_{A_i} the sum of the i level of parameter A (i = 1–4), N the repeating number of each number of each level of parameter A, f_A the degree of freedom of parameter A, V_A the variance of parameter A, F_{A_0} the F-test value of parameter A. F-test is a powerful technique to observe the important process parameters of the influence of tool rotational speed and its content on the tensile strength under different conditions. F-value is simply a ratio of the mean of the squared deviations to the mean of squared error. Generally, larger F value, the effect is

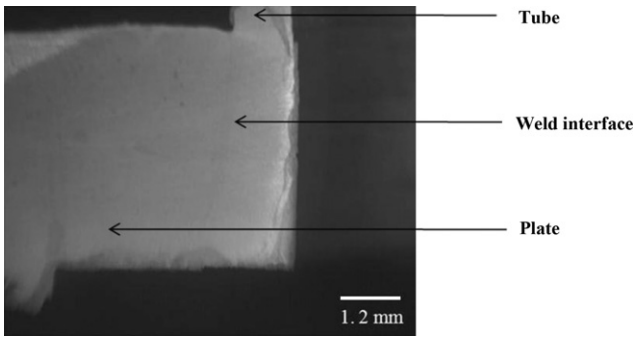

Fig. 9. Macrostructure of weld joint obtained by FWTPET process.

greater on the deformation. This analysis was undertaken for a level of significance of 5%, and confidence level of 95%.

6. Results and discussion

The main objective of the present work is to study, predict, and optimize the strength behavior due to the effect of tool rotational speed, pin clearance and shoulder diameter on joints made by FWTPET process under different conditions using BPNN and GA. The macrostructures of the weld obtained with tool rotational speed, pin clearance and shoulder diameter of 1030 rpm, 1 mm and 30 mm respectively is shown in Fig. 9. The macrostructural observation reveals a better weld interface between the tube and the tube plate. A careful observation leads to an inference that the weld interface does not possess defects such as crack, porosity etc. so that better bonding takes place between the tube and the tube plate. The microstructures of the weld joint obtained with the process parameters (1030 rpm speed, 1 mm pin clearance and 30 mm shoulder diameter) have been analyzed at different weld zones in Fig. 10. The friction welded joints have been sectioned perpendicular to the bond line and observed using optical microscope. Typical micrographs depicting different morphology of microstructure at different zones of the friction welded joints has been presented and analyzed. Compared to the base metal, the changes in microstructure are observed obviously at weld zone interface. The grains at base metal (plate and tube) are relatively coarser. Fine grain structure has been observed in the weld zone interface. In solid state welding, especially in friction welding, due to severe deformation, the refined grain structure is observed at the weld zone which resulted in improved properties. It has been found that weld joints shown in Figs. 9 and 10 possess good bonding between tube and tube plate at the interface. When more quantity of plate material which is in plastic condition is forced through a small hole, the tube surfaces surrounding the holes may reaches plastic condition. Fig. 11 depict that the fracture has been occurred in the weld zone. Hence, a maximum tensile strength has been achieved by the FWTPET process.

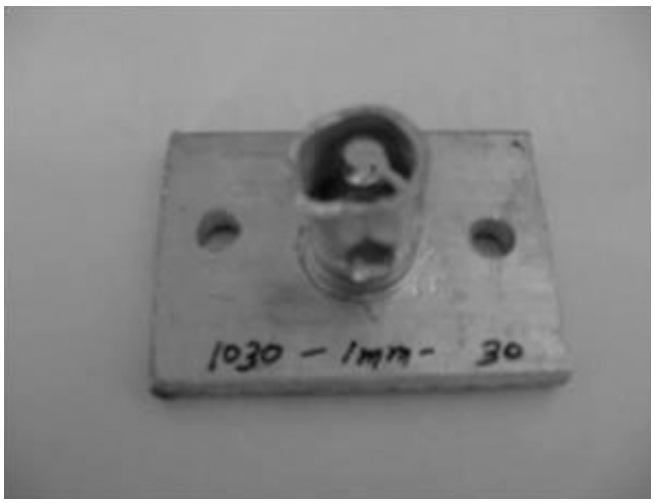

Fig. 11. Fractured tensile test sample.

6.1. Investigation on the performance of BPNN

The performance capability of each network has been examined based on the correlation coefficient, error distribution, and convergence of entire dataset within specified error range between the network predictions and the experimental values using the test and entire dataset. In order to decide the optimum structure of neural network, the rate of convergence error was checked by

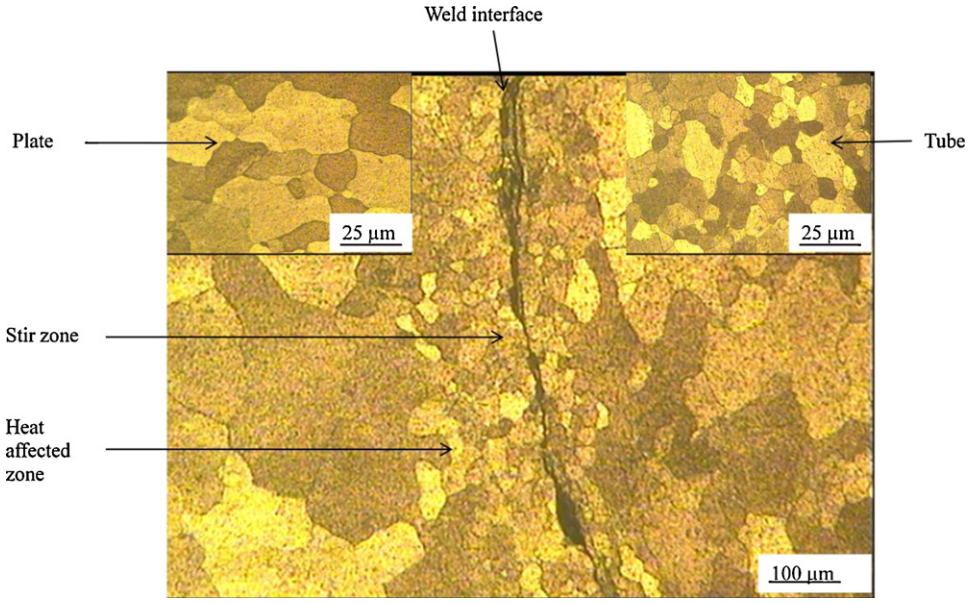

Fig. 10. Microstructure of different weld zones obtained by FWTPET process.

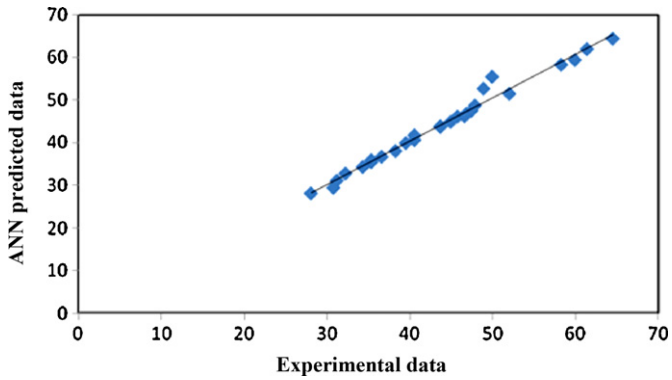

Fig. 12. Correlation between the predicted values of the neural network model and the experimental data for prediction of the tensile strength using the entire dataset of FWTPET process.

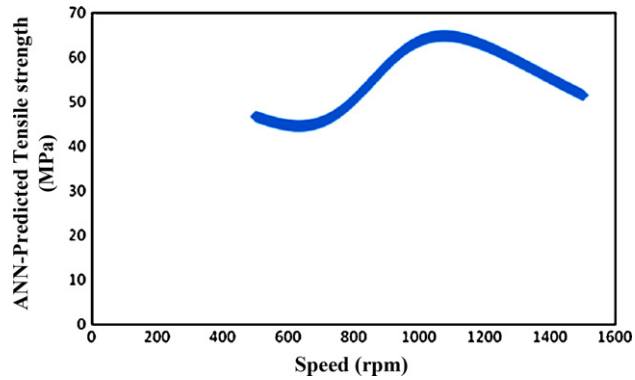

Fig. 13. Variation of the tensile strength as a function of speed and predicted by neural network model 3–3–1.

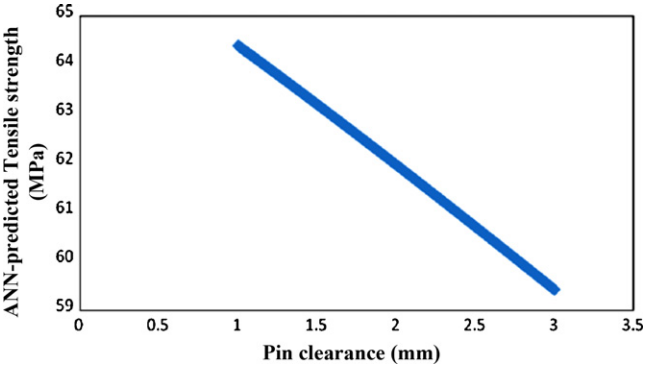

Fig. 14. Variation of the tensile strength as a function of pin clearance and predicted by neural network model 3–3–1.

changing the number of hidden neurons and number of hidden layers.

From Table 4, it is identified that the network with single hidden layer of 25 neurons has yielded correlation coefficient of 0.7404 and mean error of 4.4740% which means the error distribution was uniform. But it was observed that only 66.66% of entire dataset are within ±4% error (Table 4). Further increase of neurons in the single hidden layer (beyond 25), has lead to nonuniform error distribution (Tables 4 and 5). Hence, it has been decided to select two hidden layers and number of neurons in each hidden layer is varied to generate optimum result. It was inferred from Table 4 that the network with up to 10 neurons in each hidden layer has produced the worst performance for each of the output parameters (3–10–10–1). The error distribution has not been varied uniformly in the second hidden layer compared to the single hidden layer. It is also observed that the architectures 3–2–1, 3–4–1 does not possess much difference in the mean correlation coefficient than previous architecture; they are not selected as optimum architecture, because the mean prediction error as well as the error distribution, maximum value of error, minimum value of error were observed as high which can be obviously seen from Table 4.Though the architecture 3–10–1 has produced the least mean prediction error of 0.014496% among the tested architectures, which indicates the uniform error distribution with mean correlation coefficient of 0.9779, it had not been selected as an optimum one because only 70.37% of entire dataset lies within ±4% error. Hence, it has been decided and concluded that the selection of optimum architecture depends on mean error %, maximum error %, minimum error %, error distribution % (i.e. frequency of error, Table 5), correlation coefficient, and convergence of entire dataset within the expected error range. Table 6 shows the partial sample experimental data, predicted data and prediction error for the tensile strength behavior of the optimum architecture model (3–3–1). Thus, network having single hidden layers of 3 neurons in each (3–3–1), trained with Levenberg–Marquardt algorithm has been selected as the optimum network model. It is also observed that the increase in the number of neurons in the single hidden layers does not possess significant improvement on the performance of the network and then the performance is decreased. The correlation between the predicted values of the optimum neural network model and the experimental data for prediction of tensile strength using the entire datasets is shown in Fig. 12. The error distribution in terms of number of error frequency and convergence of percentages of the entire dataset within permissible range (±4%) of the selected network architectures for the purpose of comparison is presented in Table 5. From Table 4, it was evaluated and found that the optimum network model of 3–3–1 has mean prediction error of −0.85102% on the entire dataset. The result shows that 88.88% of the entire dataset have the percentage error ranging within ±4%.

This demonstrated that the developed model has high accuracy for predicting the tensile strength behavior of the FWTPET process. The variation of the tensile strength predicted by the ANN model for selected sample is presented in Figs. 13–15.

Based on the optimized network parameters, the ANN model has been developed to predict tensile strength behavior of FWTPET process. From Table 6 a good agreement has been made between experimentation and prediction 3–3–1 in the case of architecture for FWTPET process. It is obviously observed from Figs. 13–15, the prediction of tensile strength behavior is possible. It has been concluded that the ANN model could predict the exact behavior. An observation from Fig. 13 reveals that the strength behavior initially starts at low and gradually increased up to optimum speed. In the initial condition, the tensile strength has been decreased due to improper heat or friction created between the tube and the tube plate. But, the increase of speed up to optimum level of FWTPET

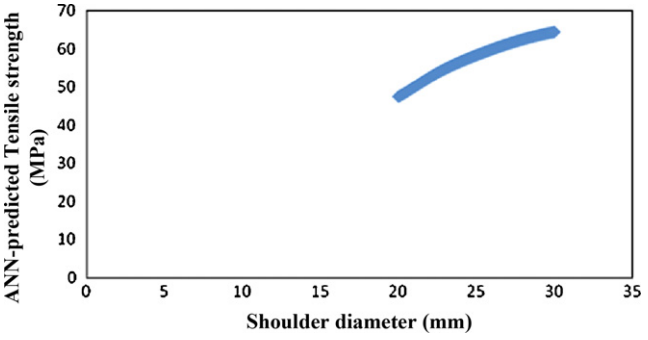

Fig. 15. Variation of the tensile strength as a function of shoulder diameter and predicted by neural network model 3–3–1.

Table 4
Correlation coefficient between the network predictions and the experimental values using the test and the entire dataset of different network architecture and trained output parameters for FWTPET process.

Network architecture	Dataset	Tensile strength (MPa) correlation coefficients	Network performance during training		Maximum error	Minimum error	Mean prediction error (%)
			MSE	Status of convergence			
3–1–1	Test	0.9748	1.45E−01	Not converged	26.8840	−41.8062	−9.38368
	Entire	0.9955	1.19E−01		22.1505	−37.3005	−5.49848
3–2–1	Test	0.9892	1.44E−03	Converged at 12 epochs	4.7879	−10.3805	−3.54104
	Entire	0.9880	1.44E−03		4.78748	−10.3796	−1.19461
3–3–1	Test	0.9911	4.34E−04	Converged at 9 epochs	3.4999	−11.4831	−2.07076
	Entire	0.9912	3.17E−04		4.3145	−11.0577	−0.85102
3–4–1	Test	0.9870	2.17E−02	Converged at 9 epochs	18.5457	−6.9815	4.554242
	Entire	0.9886	1.59E−04		5.3573	−10.8740	−1.11912
3–5–1	Test	0.9667	2.56E−31	Converged at 9 epochs	0.2598	−16.9180	−5.60739
	Entire	0.9675	1.64E−23		71.7930	−62.9882	7.379999
3–6–1	Test	0.9745	1.94E−30	Converged at 9 epochs	12.4508	−95.9913	29.07373
	Entire	0.9751	1.63E−19		19.2306	−16.3261	−0.40913
3–7–1	Test	0.9877	4.13E−30	Converged at 9 epochs	4.9102	−9.94219	−4.53728
	Entire	0.9882	8.34E−25		6.49306	−7.72559	−0.31129
3–8–1	Test	0.9293	1.56E−26	Converged at 9 epochs	4.5487	−28.9386	−8.2376
	Entire	0.9301	1.16E−22		1.2993	−14.7372	−2.40469
3–9–1	Test	0.9674	1.07E−20	Converged at 8 epochs	9.4031	−19.1025	−2.56832
	Entire	0.9688	6.27E−31		92.4608	−112.6860	7.236741
3–10–1	Test	0.9764	2.20E−23	Converged at 7 epochs	16.7103	−27.2996	−9.4021
	Entire	0.9779	3.32E−29		13.0998	−20.4089	0.014496
3–11–1	Test	0.9532	6.95E−31	Converged at 7 epochs	63.5745	−93.0786	−8.10507
	Entire	0.9540	4.33E−27		28.4394	−22.8462	0.361604
3–12–1	Test	0.9564	1.06E−28	Converged at 7 epochs	9.38016	9.380161	−7.22481
	Entire	0.9578	4.26E−31		8.68942	−70.9447	−9.18749
3–13–1	Test	0.9272	5.57E−28	Converged at 6 epochs	8.39842	−19.9250	−7.5329
	Entire	0.9288	1.56E−21		48.5761	−102.1810	−6.58963
3–14–1	Test	0.9310	1.55E−31	Converged at 6 epochs	48.5218	−47.6360	−7.12558
	Entire	0.9323	2.11E−22		29.0681	−26.0910	0.220132
3–15–1	Test	0.9125	7.12E−22	Converged at 5 epochs	31.8365	−9.02175	9.031413
	Entire	0.9140	4.19E−31		77.4847	−100.3850	0.62542
3–16–1	Test	0.9008	3.20E−32	Converged at 5 epochs	47.9534	−30.0105	13.29538
	Entire	0.9014	1.50E−29		43.2835	−43.1796	−2.17103
3–17–1	Test	0.8990	1.91E−25	Converged at 5 epochs	31.4766	−47.9363	5.850678
	Entire	0.8996	3.02E−24		20.1991	−47.7512	−1.34535
3–18–1	Test	0.8876	2.64E−29	Converged at 5 epochs	40.7208	−17.3804	5.72257
	Entire	0.8882	4.36E−31		15.6054	−35.8496	−2.307
3–19–1	Test	0.8502	1.62E−31	Converged at 5 epochs	23.648	−14.3071	8.14365
	Entire	0.8565	5.18E−30		117.228	−2.63875	11.1833
3–20–1	Test	0.8422	1.80E−32	Converged at 5 epochs	67.5674	−56.5418	0.1594
	Entire	0.8448	1.68E−31		21.7051	−27.4322	−1.7137
3–21–1	Test	0.8214	2.22E−31	Converged at 5 epochs	90.1819	−45.9777	14.4022
	Entire	0.8220	2.08E−31		34.2452	−49.6421	1.0901
3–22–1	Test	0.8110	1.86E−32	Converged at 5 epochs	38.8656	−22.0609	5.2863
	Entire	0.8122	2.08E−31		44.1794	−48.4986	2.4619
3–23–1	Test	0.7940	1.06E−31	Converged at 5 epochs	54.6090	−25.9292	17.2854
	Entire	0.7952	2.34E−31		59.6384	−50.1295	0.2246
3–24–1	Test	0.7415	1.45E−31	Converged at 5 epochs	16.6470	−81.9572	−32.4454
	Entire	0.7422	1.04E−27		36.2881	−96.6986	−4.6539
3–25–1	Test	0.7399	3.81E−22	Converged at 5 epochs	66.3985	−46.0324	7.6529
	Entire	0.7404	9.41E−22		67.9456	−54.3843	4.4740
3–1–1–1	Test	0.6479	1.19E−01	Not converged	19.3000	−37.3003	−12.4899
	Entire	0.6485	1.19E−01		22.1397	−37.2985	−5.5014
3–2–2–1	Test	0.6215	1.36E−01	Not converged	27.1186	−50.1559	−9.4932
	Entire	0.6232	1.12E−01		24.0015	−30.7654	−3.2868
3–3–3–1	Test	0.5895	1.00E−01	Not converged	40.9002	−59.4976	−1.31201
	Entire	0.5994	1.12E−01		37.98	−62.8430	2.8777
3–4–4–1	Test	0.5786	5.89E−02	Not converged	16.1788	−54.0164	−14.2546
	Entire	0.5774	5.31E−04		4.58344	−20.8894	−2.4899
3–5–5–1	Test	0.5680	3.03E−04	Not converged	10.3211	−29.1241	−4.7493
	Entire	0.5684	6.06E−04		5.56463	−17.2437	−1.0845
3–6–6–1	Test	0.5337	4.44E−01	Not converged	38.6289	−76.1190	−19.820
	Entire	0.5345	5.46E−04		6.97258	−27.1344	−2.5852
3–7–7–1	Test	0.5330	4.06E−05	Not converged	31.9022	−25.0317	1.55008
	Entire	0.5332	6.13E−04		20.4344	−102.55	−3.4799
3–8–8–1	Test	0.5240	3.83E−06	Not converged	17.1729	−37.2464	−8.0008
	Entire	0.5248	5.44E−05		42.5461	−81.7648	3.21869
3–9–9–1	Test	0.5238	7.14E−01	Not converged	12.9222	−82.3396	−40.0977
	Entire	0.5240	5.74E−05		39.4703	−63.2794	0.3138
3–10–10–1	Test	0.5224	6.51E−01	Not converged	20.5990	−99.969	−41.2036
	Entire	0.5225	1.07E−10		42.5328	−78.9699	−0.40311

Table 5
Comparison of the error distribution in terms of the error frequency of the entire dataset for the selected network architecture.

Network architecture	Number of error frequency						
	3–2–1	**3–3–1**	3–5–1	3–10–1	3–25–1	3–5–5–1	3–10–10–1
Error frequency range (%)							
<−50	0	0	1	0	1	0	0
−50 to −45	0	0	0	0	1	0	0
−45to −40	0	0	0	0	0	0	0
−40to −35	0	0	0	0	0	0	0
−35 to −30	0	0	0	0	0	0	0
−30 to −25	0	0	0	0	0	0	0
−25 to −20	0	0	0	1	0	0	1
−20 to −16	0	0	0	0	1	0	0
−16 to −12	0	0	1	0	0	0	1
−12 to −8	1	1	0	1	0	0	1
−8 to −4	2	1	0	1	1	0	0
−4 to −4 (% of data within this range)	23(85.18)	**24 (88.88)**	19(70.37)	19(70.37)	18(66.66)	16(59.25)	11(40.74)
+4 to +8	1	1	0	4	1	0	3
+8 to +12	0	0	1	2	0	1	5
+12 to +16	0	0	1	1	0	2	0
+16 to +20	0	0	0	0	0	0	0
+20 to +25	0	0	0	0	1	1	1
+25 to +30	0	0	0	0	1	1	1
+30 to +35	0	0	0	0	0	1	1
+35 to +40	0	0	0	0	1	0	1
+40 to +45	0	0	0	0	1	2	0
+45 to +50	0	0	0	0	0	0	0
>+50	0	0	4	0	1	0	0

Bold indicates optimal architecture.

process has created sufficient heat between the tube and the tube plate. In this condition, metal has reached plastic condition due to friction so that better bonding takes place between the tube and the tube plate. Then the tensile strength has been improved to the optimum level of speed. However, beyond the optimum level of speed, the tensile strength is found to decrease. This phenomenon is due to excessive deformation of metal which may leads to defects formation. Fig. 14 shows that the strength behavior as a function of pin clearance. The pin clearance is the gap that exists between the tube and the tube plate of FWTPET process. Better strength behavior is achieved with the reduced pin clearance. As the metal reaches plastic condition, the pin surface will act as an anvil and offer better compaction. As the shoulder diameter is increased, the heat generation rate will be more. Hence, an improved joint strength can be achieved and presented in Fig. 15 [19].

6.2. Optimized results using Genetic Algorithm

Fig. 16 depicts the convergence result obtained in GA. Table 7 presents the optimized parameters for obtaining maximum tensile strength. Based on the optimum value, validation experiment has been conducted using the feasible input parameters. There

Table 6
Partial sample predicted data from testing results and experimental data, and prediction error of the 3–3–1 network model.

Experimental input			Experimental output		
Speed (rpm)	Pin clearance (mm)	Shoulder diameter (mm)	Tensile strength (Mpa)	Predicted data	Percentage of error
500	1	20	31.22	31.14	0.08
500	1	25	35.39	35.94	−0.55
500	1	30	46.83	46.77	0.06
500	2	20	30.81	29.48	1.33
500	2	25	34.35	34.35	0.00
500	2	30	43.71	43.78	−0.07
500	3	20	28.10	28.17	−0.07
500	3	25	32.27	32.83	−0.56
500	3	30	40.59	40.65	−0.06
1030	1	20	47.46	47.49	−0.03
1030	1	25	58.29	58.31	−0.02
1030	1	30	64.53	64.39	0.14
1030	2	20	45.79	46.17	−0.38
1030	2	25	49.96	55.48	−5.52
1030	2	30	61.41	61.96	−0.55
1030	3	20	44.96	44.94	0.02
1030	3	25	48.92	52.71	−3.79
1030	3	30	59.95	59.42	0.53
1500	1	20	38.30	38.09	0.21
1500	1	25	43.72	43.84	−0.12
1500	1	30	52.04	51.52	0.52
1500	2	20	36.64	36.74	−0.1
1500	2	25	40.59	41.77	−1.18
1500	2	30	47.88	48.76	−0.88
1500	3	20	35.39	35.48	−0.09
1500	3	25	39.55	39.93	−0.38
1500	3	30	46.63	46.23	0.4

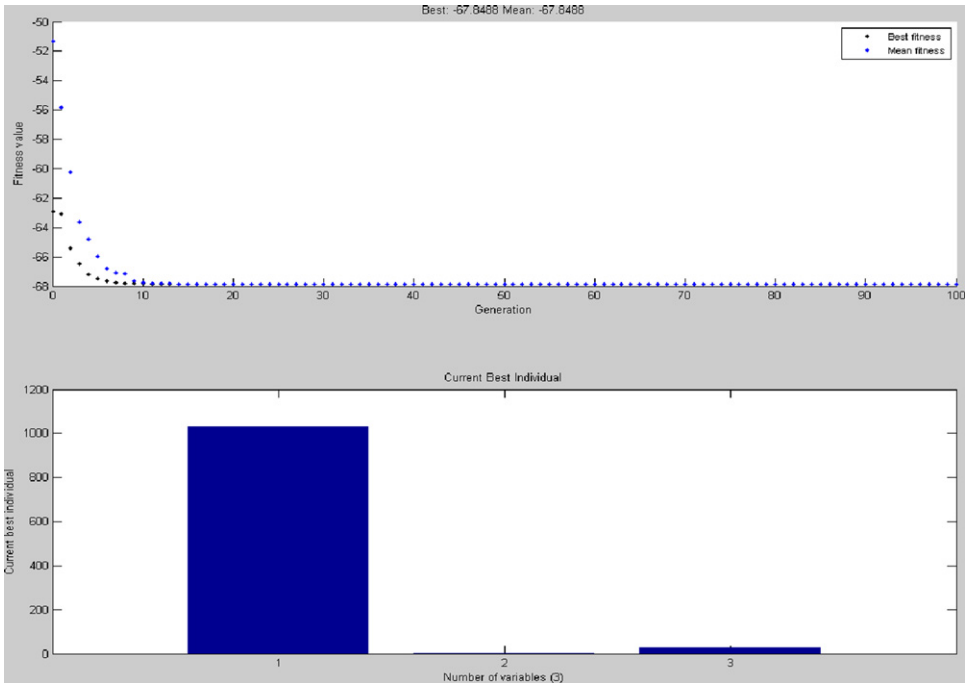

Fig. 16. Screenshot depicting the convergence result obtained using GA.

Table 7
Optimized results.

	Tool rotational speed (rpm)	Pin clearance (mm)	Shoulder diameter (mm)	Tensile strength (MPa)
GA	1031.47419	1.00002	29.28207	67.8488
Experimental value	1030	1	30	64.53

Table 8
Results of the statistical analysis of variance (ANOVA).

Source	DF	SS	MS	*F*	*P*	Percentage of contribution (%)
Tool rotational speed	2	1421.23	710.61	335.82	0.000	57.95
Pin clearance	2	97.92	48.96	23.14	0.000	3.99
Shoulder diameter	2	890.88	445.44	210.51	0.000	36.33
Error	20	42.32	2.12			1.72
Total	26	2452.34				100

DF, degree of freedom; SS, sum of squares; MS, mean squares; *F*, statistical test; *P*, statistical value.

has been a narrow deviation between theoretically predicted and experimentally obtained values for tensile strength which confirm the practical applicability of GA to FWTPET process. Hence a maximum possible strength has been achieved by the optimization study. The strength achieved using optimized process parameters is 64.53 MPa (1030 rpm, 1 mm pin clearance and 30 mm shoulder diameter).

6.3. Quantitative and statistical analysis

Quantitative and statistical analysis of variance (ANOVA) was performed to understand the influence of the each parameter on the strength behavior of FWTPET process. It helps to determine the effect of individual input parameters on output parameters. The results of ANOVA are presented in Table 8. Based on the results presented in Table 8, tool rotational speed is found to be the most influencing parameter with 57.95% contribution followed by shoulder diameter (36.33%) and pin clearance (3.99%) and is shown in Fig. 17. The main effects plot generated by MINITAB software pertaining to ANOVA is shown in Fig. 18. It can be inferred that higher tensile strength could be obtained when the speed are optimum, pin clearance are low and shoulder diameter is large. However at very low speeds, heat generation and joint strength is found to be poor.

6.4. Industrial value/relevance of the approach

FWTPET process possess high potential for applications in several industrial sectors such as automotive, aerospace, electronics, boiler components heat exchangers, pressure vessels, etc., In these industrial sectors, the application of ANN & GA enables the identification of optimal process architecture. Also,

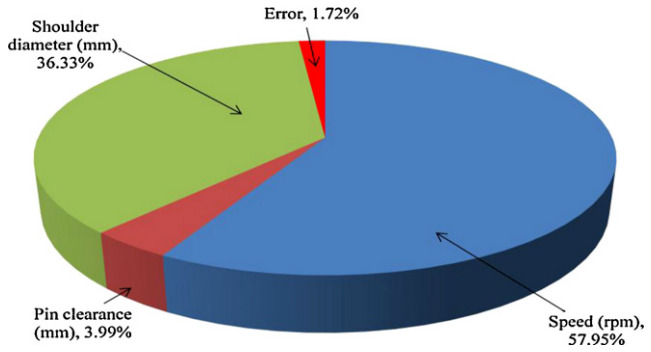

Fig. 17. Contribution in percentage of FWTPET process parameters.

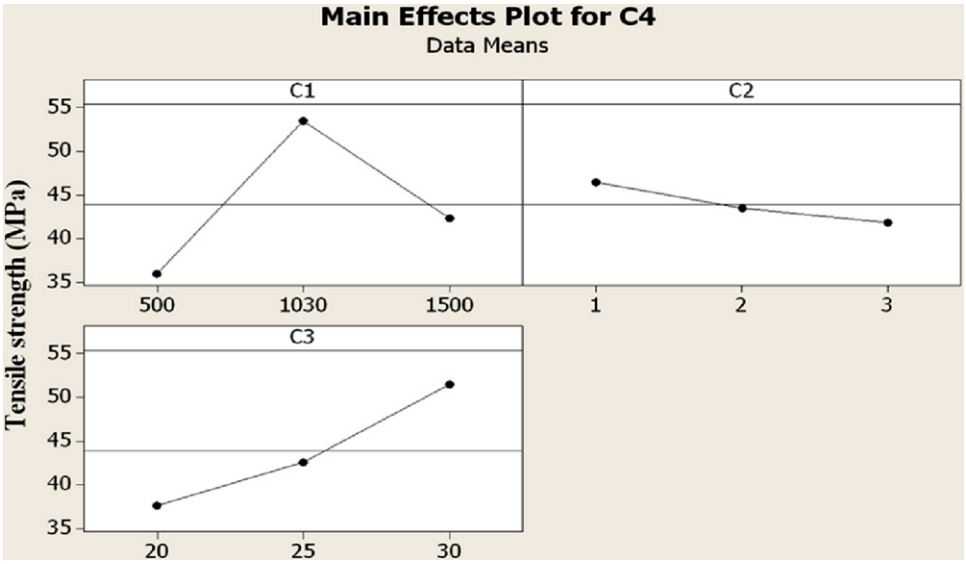

Fig. 18. Main effects plot generated by MINITAB software.

the application of statistical techniques enables the determination of contribution of process parameters towards enhancing process effectiveness.

7. Conclusions

In this study, FWTPET process has been used to join tube to tube plate which is a new and innovative process and has wider applications. In order to reduce fabrication cost, researchers have been exploring the newer welding process to improve the joint properties. This process is capable of producing high quality tube to tube plate weld joints with enhanced mechanical and metallurgical properties.

ANN has been used in this study; Based upon the correlation coefficient, error distribution, and convergence 35 different BPNN architectures are trained/analyzed using the experimental data until an optimum architecture has been identified.

Out of the different multi-layer BPNN architectures trained, the BPNN with single hidden layers having 3 neurons trained with Levenberg–Marquardt algorithm has been observed to be the optimum network model (3–3–1).

A sound performance has been achieved with the neural network model, with a good correlation coefficient (between the predicted and experimental values), high uniform error distribution and convergence of entire dataset within the permissible error range.

The optimal architecture derived from ANN has been used to predict the output parameters. The predicted output parameters from ANN and input parameters have been optimized using GA. The optimized parameters obtained from GA have been compared with experimental values. There is a minimal deviation between theoretically optimized and experimentally obtained process parameters.

Statistical technique ANOVA has been employed to determine the percentage contributions of the process parameters; speed possess highest contribution (57.95%) followed by the shoulder diameter (36.33%) and pin clearance (3.99%).

Acknowledgments

The authors are grateful to the Central workshop, National Institute of Technology, Tiruchirappalli, Tamil Nadu, India for extending the facilities to carry out this investigation. The authors also wish to express their sincere thanks to Ministry of Human Resource Development (MHRD), Government of India for the financial support to carry out this investigation.

References

[1] S. Muthukumaran, A process for friction welding of tube to tube sheet or a plate by adopting an external tool, Indian patent application no. 189/KOL/06 filed on 07-03-2006, Patent No. 217446 (granted on 26.03.08).
[2] S. Senthil Kumaran, S. Muthukumaran, S. Vinodh, Struct. Multidisc. Optim. 42 (2010) 449–457.
[3] S. Senthil Kumaran, S. Muthukumaran, S. Vinodh, Inter. J. Eng. Sci. Technol. 2 (2010) 109–117.
[4] A.K. Lakshminarayanan, V. Balasubramanian, Trans. Nonferrous Met. Soc. China 18 (2008) 548–554.
[5] P. Sathiya, S. Aravindan, A. Noorul Haq, K. Paneerselvam, J. Mater. Process. Technol. 209 (2009) 2576–2584.
[6] S. Muthukumaran, C. Pradeep, C. Vijaya Kumar, S. Senthil Kumaran, International Welding Symposium, 2k10, 2010, pp. 235–239.
[7] A.K. Lakshminarayanan, V. Balasubramanian, Trans. Nonferrous Met. Soc. China 19 (2009) 9–18.
[8] E.M. Bezerra, A.C. Ancelotti, L.C. Pardini, J.A.F.F. Rocco, K. Iha, C.H.C. Ribeiro, Mater. Eng. A 464 (2007) 177–183.
[9] W.C. Chen, G.L. Fu, P.H. Tai, W.J. Deng, Exp. Syst. Appl. 36 (2009) 1114–1122.
[10] S. Malinov, W. Sha, J.J. McKeown, Comput. Mater. Sci. 21 (2001) 375–394.
[11] H. Demuth, M. Beale, Neural Network Toolbox User's Guide, Version 4 (Release12), The Mathworks, Inc., 2000.
[12] A.K. Singh, S.S. Panda, S.K. Pal, D. Chakraborty, Int. J. Adv. Manuf. Technol. 28 (2006) 456–462.
[13] E.O. Ezugwu, D.A. Fadare, J. Bonney, W.F. Sales, R.B. Da Silva, Int. J. Mach. Tool Manuf. 45 (2005) 1375–1385.
[14] N.S. Reddy, J. Krishnaiah, S.G. Hong, J.S. Lee, Mater. Sci. Eng. A (1–2) (2008) 93–105.
[15] S.N. Singh, L. Srivastava, J. Sharma, J. Elec. Power Syst. Res. 53 (2000) 197–205.
[16] K. Paneerselvam, S. Aravindan, A. Noorul Haq, J. Adv. Manuf. Technol. 42 (2009) 669–677.
[17] J.H. Holland, Adaptation in Natural and Artificial Systems, University of Michigan Press, Ann Arbor, 1975.
[18] D.E. Goldberg, Genetic Algorithms in Search, Optimization and Machine Learning, Addison-Wesley, New York, 1989.
[19] S. Muthukumaran, International Welding Symposium 2k10, 2010, pp. 241–245.